A broadened classical master equation approach for treating electron-nuclear coupling in non-equilibrium transport

Cite as: J. Chem. Phys. **148**, 102317 (2018); https://doi.org/10.1063/1.4992784
Submitted: 26 June 2017 • Accepted: 11 October 2017 • Published Online: 20 November 2017

Wenjie Dou, Christian Schinabeck, Michael Thoss, et al.

A broadened classical master equation approach for treating electron-nuclear coupling in non-equilibrium transport

Wenjie Dou,[1] Christian Schinabeck,[2] Michael Thoss,[2,3] and Joseph E. Subotnik[1]
[1]*Department of Chemistry, University of Pennsylvania, Philadelphia, Pennsylvania 19104, USA*
[2]*Institute for Theoretical Physics and Interdisciplinary Center for Molecular Materials, University Erlangen-Nürnberg, Staudtstr. 7/B2, D-91058 Erlangen, Germany*
[3]*Institute of Physics, University of Freiburg, Hermann-Herder-Strasse 3, D-79104 Freiburg, Germany*

(Received 26 June 2017; accepted 11 October 2017; published online 20 November 2017)

We extend the broadened classical master equation (bCME) approach [W. Dou and J. E. Subotnik, J. Chem. Phys. **144**, 024116 (2016)] to the case of two electrodes, such that we may now calculate non-equilibrium transport properties when molecules come near metal surfaces and there is both strong electron-nuclear and strong metal-molecule coupling. By comparing against a numerically exact solution, we show that the bCME usually works very well, provided that the temperature is high enough that a classical treatment of nuclear motion is valid. Finally, in the low temperature (quantum) regime, we suggest a means to incorporate broadening effects in the quantum master equation (QME). This bQME works well for fairly low temperatures. *Published by AIP Publishing.*
https://doi.org/10.1063/1.4992784

I. INTRODUCTION

Single-molecule junctions have gained a lot of interest over the past few decades[1–3] where many interesting phenomena have been found, such as Coulomb blockades,[4–7] Kondo effects,[8–12] and Franck-Condon blockades.[13–16] It is now well known that electron-nuclear couplings can play an important role in many molecular junction transport processes,[17,18] leading to heating,[19–23] nonadiabatic effects,[24–27] enhanced current fluctuations,[28–30] hysteresis or switching,[31–34] negative differential resistance,[35–39] and current induced chemistry.[40–44] To understand these phenomena, theoretical insight can be gained from a non-equilibrium Green's function (NEGF)[45–55] formalism, the quantum master equation (QME),[39,45,56–58] and semiclassical methods.[59–61] At the same time, numerically exact methods including numerical renormalization group (NRG) theory,[62] quantum Monte Carlo (QMC),[63–66] the multilayer multiconfiguration time-dependent Hartree (ML-MCTDH) approach[67,68] and the hierarchical quantum master equation (HQME)[69–71] allow one to benchmark the former approximate tools.

For the most part, in order to model a realistic molecule present in a junction or near metal surfaces, many nuclear degrees of freedom (DoFs) are involved, such that a quantum treatment of all of the nuclear motion is challenging. That being said, a semiclassical treatment is possible for a large number of low frequency modes at relatively high temperature. Motivated by such a consideration, over the past two years, two of us have investigated a classical master equation (CME) approach to describe the semiclassical dynamics of coupled electron-nuclear motion for molecules near metal surfaces.[72–74] Because it is based on perturbation theory, a straightforward, undressed CME works well only for weak molecule-metal couplings. However, this CME can successfully be then mapped onto a Fokker-Planck (FP) equation through an adiabatic transformation.[75] By comparing the resulting FP equation against the standard form of Langevin dynamics produced by a non-equilibrium Green's function (NEGF) expansion (which is based on the idea of small nuclear velocities),[47] it has been previously demonstrated that for the case of a single metal surface, one can modify the potential energy surfaces to incorporate broadening effects in an *ad hoc* manner. The resulting broadened CME (bCME) successfully extrapolates between both weak and strong molecule-metal couplings.[76]

In the present paper, we will now extend the previous results to the case of two electrodes so that we may calculate non-equilibrium transport properties. Following a similar procedure as for the case of one electrode, we will derive a Fokker-Planck equation via an adiabatic approximation. The corresponding friction and random force will agree with previously published results,[47] provided broadening can be disregarded. Note that in the non-equilibrium case, i.e., the case of two different Fermi levels on the different metals, the friction and random force will not obey the second fluctuation-dissipation theorem, resulting in heating of the nuclear modes. A simple broadening scheme will be introduced to calculate transport properties and we will benchmark our results against numerically exact results from the HQME and demonstrate strong agreement across nonadiabatic and adiabatic regimes (as long as the nuclei are classical).

To address the low temperature (quantum) limit, a similar (and simple) broadening scheme for the QME is introduced (which we will denote as a bQME). The results from the bQME recover bCME results at relatively high temperature and agree well with numerically exact HQME solutions at fairly low temperature. That being said, however, in the case of very low temperature, both the bCME and the bQME show deviations from the exact HQME results.

We organize our paper as follows. In Sec. II, we review the CME and introduce the bCME. In Sec. III, we briefly review the QME and introduce the bQME. In Sec. IV, we discuss the numerical exact solutions from HQME. We plot results in Sec. V and conclude in Sec. VI.

II. BROADENED CLASSICAL MASTER EQUATION (bCME)

A. The Anderson-Holstein (AH) model

The model we study in this paper is the generalized spinless Anderson-Holstein (AH) model, where one level d (with creation/annihilation operator $\hat{d}^\dagger/\hat{d}$) couples both to a manifold of electronic levels indexed by k (with creation/annihilation operator $\hat{c}_k^\dagger/\hat{c}_k$) and to a nuclear degree of freedom (DoF, with position/momentum operator $\hat{x}/\hat{p}$),

$$\hat{H} = h(\hat{x})\hat{d}^\dagger\hat{d} + U_0(\hat{x}) + \frac{\hat{p}^2}{2m} + \sum_{k\in \mathrm{L,R}} V_k(\hat{c}_k^\dagger\hat{d} + \hat{d}^\dagger\hat{c}_k) + \sum_{k\in \mathrm{L,R}} \epsilon_k \hat{c}_k^\dagger\hat{c}_k. \tag{1}$$

For such a model, we can define the hybridization function due to coupling to the left and right leads,

$$\Gamma^K(\epsilon) \equiv 2\pi \sum_{k\in K} V_k^2 \delta(\epsilon - \epsilon_k). \tag{2}$$

We have introduced the lead index $K = \mathrm{L,R}$ (i.e., left and right). Below, we will assume the wide-band approximation, such that Γ^K is independent of energy. For convenience, we will further define

$$\Gamma \equiv \Gamma^{\mathrm{L}} + \Gamma^{\mathrm{R}}. \tag{3}$$

B. Classical master equation

In the high temperature limit, i.e., $k_BT > \hbar\omega$ (ω is the typical frequency of the nuclear motion) and $k_BT > \Gamma$, as shown in Refs. 72 and 77, we can use a classical master equation (CME) to describe the dynamics

$$\frac{\partial}{\partial t}\rho_0(x,p,t) = -\frac{p}{m}\frac{\partial \rho_0}{\partial x} + \frac{\partial U_0}{\partial x}\frac{\partial \rho_0}{\partial p} - \frac{\Gamma}{\hbar}\bar{f}(h)\rho_0 + \frac{\Gamma}{\hbar}(1-\bar{f}(h))\rho_1, \tag{4a}$$

$$\frac{\partial}{\partial t}\rho_1(x,p,t) = -\frac{p}{m}\frac{\partial \rho_1}{\partial x} + \frac{\partial U_1}{\partial x}\frac{\partial \rho_1}{\partial p} + \frac{\Gamma}{\hbar}\bar{f}(h)\rho_0 - \frac{\Gamma}{\hbar}(1-\bar{f}(h))\rho_1, \tag{4b}$$

where $\rho_0(x,p)$ ($\rho_1(x,p)$) is the probability density for the nuclei to be located in phase space at (x,p) with energy level d being unoccupied (occupied). In the above equations, we have defined

$$U_1(x) = U_0(x) + h(x), \tag{5a}$$

$$\bar{f}(h) = \frac{1}{\Gamma}(\Gamma^L f^L(h) + \Gamma^R f^R(h)), \tag{5b}$$

where $f^K(h) = (e^{(h(x)-\mu_K)/k_BT} + 1)^{-1}$ is the Fermi function of lead K (μ_K is the corresponding chemical potential). Below, for brevity, we will abbreviate $\bar{f}(h)$ as $\bar{f}$. Physically, if there is no nuclear motion, $\bar{f}(h)$ would be the equilibrium population of the level at position x.

Note that the CME [Eq. (4)] is valid in the high temperature limit: (1) $k_BT > \hbar\omega$, such that a classical treatment of the nuclei with the CME is feasible; (2) $k_BT > \Gamma$, such that all broadening effects can be disregarded. Below, similar to Refs. 76 and 78, we will modify our CME to partially incorporate broadening effects. To achieve such a modification, we require an adiabatic transformation.

C. Adiabatic transformation and Fokker-Planck equation

We start our adiabatic transformation by defining new density probabilities $A(x,p,t)$ and $B(x,p,t)$,

$$\rho_0(x,p,t) \equiv (1-\bar{f})A(x,p,t) + B(x,p,t), \tag{6a}$$

$$\rho_1(x,p,t) \equiv \bar{f}A(x,p,t) - B(x,p,t). \tag{6b}$$

These new definitions imply that $A(x,p) \equiv \rho_0(x,p) + \rho_1(x,p)$ is the total probability density at (x,p) and $B \equiv \bar{f}\rho_0 - (1-\bar{f})\rho_1$ are the fluctuations from equilibrium. Together with the CME [Eq. (4)], we can easily recover the equation of motion (EOM) for A and B,

$$\frac{\partial}{\partial t}A(x,p,t) = -\frac{p}{m}\frac{\partial A}{\partial x} + (\frac{\partial U_0}{\partial x} + \bar{f}\frac{\partial h}{\partial x})\frac{\partial A}{\partial p} - \frac{\partial h}{\partial x}\frac{\partial B}{\partial p}, \tag{7a}$$

$$\frac{\partial}{\partial t}B(x,p,t) = -\frac{p}{m}\frac{\partial B}{\partial x} + (\frac{\partial U_0}{\partial x} + (1-\bar{f})\frac{\partial h}{\partial x})\frac{\partial B}{\partial p} + \frac{p}{m}A\frac{\partial \bar{f}}{\partial x} - \bar{f}(1-\bar{f})\frac{\partial h}{\partial x}\frac{\partial A}{\partial p} - \frac{\Gamma}{\hbar}B. \tag{7b}$$

As argued in Refs. 75, 76, and 79, in the adiabatic limit, i.e., when the nuclear motion is slow compared with electronic transition ($\Gamma > \hbar\omega$), we approximate Eq. (7b) as

$$\frac{\Gamma}{\hbar}B \approx \frac{p}{m}A\frac{\partial \bar{f}}{\partial x} - \bar{f}(1-\bar{f})\frac{\partial h}{\partial x}\frac{\partial A}{\partial p}. \tag{8}$$

When plugging the above equation into Eq. (7a), we get a closed EOM for A,

$$\frac{\partial}{\partial t}A(x,p,t) = -\frac{p}{m}\frac{\partial A}{\partial x} - F_{pmf}(x)\frac{\partial A}{\partial p} + \gamma_e(x)\frac{\partial}{\partial p}(\frac{p}{m}A) + D_e(x)\frac{\partial^2 A}{\partial p^2}. \tag{9}$$

We remind the reader that Eq. (9) is a Fokker-Planck equation for the total density probability A (i.e., $A \equiv \rho_0 + \rho_1$ is the density for both electronic states combined). The corresponding mean force F_{pmf}, electronic friction γ_e, and correlation of the random force D_e are given by

$$F_{pmf}(x) = -\frac{\partial U_0}{\partial x} - \frac{\partial h}{\partial x}\bar{f}, \tag{10a}$$

$$\gamma_e(x) = -\frac{\hbar}{\Gamma}\frac{\partial \bar{f}}{\partial x}\frac{\partial h}{\partial x}, \tag{10b}$$

$$D_e(x) = \frac{\hbar}{\Gamma}\bar{f}(1-\bar{f})(\frac{\partial h}{\partial x})^2. \tag{10c}$$

We note that if $\mu_{\mathrm{L}} = \mu_{\mathrm{R}}$, then we have $\frac{\partial \bar{f}}{\partial x} = -\beta\bar{f}(1-\bar{f})\frac{\partial h}{\partial x}$, such that $D_e = k_BT\gamma_e$, i.e., the second fluctuation-dissipation

theorem is satisfied. By contrast, when a voltage is applied to the leads, such that $\mu_L \neq \mu_R$, $D_e = k_B T \gamma_e$ does not hold any longer. Note also that Eq. (10) agree with other previously published results (for example, Ref. 47), when level broadening can be disregarded (i.e., $k_B T > \Gamma$).

D. Incorporating broadening effects

In Ref. 47, using a velocity expansion, the NEGF formalism gives a slightly different mean force [versus Eq. (10a)],

$$\tilde{F}_{pmf}(x) = -\frac{\partial U_0}{\partial x} - \frac{\partial h}{\partial x}\bar{n}(h), \tag{11}$$

where we have defined

$$\bar{n}(h) = \int \frac{d\epsilon}{2\pi} \frac{\Gamma}{(\Gamma/2)^2 + (\epsilon - h(x))^2} \bar{f}(\epsilon). \tag{12}$$

[Again, we will abbreviate $\bar{n}(h)$ as $\bar{n}$.]

We emphasize that Eq. (11) includes broadening effects. To incorporate such effects into our EOM, we must replace the mean force F_{pmf} [in Eq. (10a)] by the broadened mean force $\tilde{F}_{pmf}$,

$$\frac{\partial}{\partial t}A(x,p,t) = -\frac{p}{m}\frac{\partial A}{\partial x} + (\frac{\partial U_0}{\partial x} + \bar{n}\frac{\partial h}{\partial x})\frac{\partial A}{\partial p} - \frac{\partial h}{\partial x}\frac{\partial B}{\partial p}. \tag{13}$$

Now, the key issue becomes if and how to modify the mean force for B. In Ref. 76, the mean force for B was not altered. In Ref. 78, in order to make the final bCME simpler (as shown below), we modify the mean force for B as follows:

$$\frac{\partial}{\partial t}B(x,p,t) = -\frac{p}{m}\frac{\partial B}{\partial x} + \left(\frac{\partial U_0}{\partial x} + (1 + \bar{n} - 2\bar{f})\frac{\partial h}{\partial x}\right)\frac{\partial B}{\partial p} + \frac{p}{m}A\frac{\partial \bar{f}}{\partial x} - \bar{f}(1-\bar{f})\frac{\partial h}{\partial x}\frac{\partial A}{\partial p} - \frac{\Gamma}{\hbar}B. \tag{14}$$

Empirically, Eqs. (7b) and (14) [together with Eq. (13)] give almost identical results for a large regime of parameters.[78] Hence, for simplicity, we will use Eq. (14) instead of Eq. (7b).

Finally, using the modified EOM for A and B [Eqs. (13) and (14)], together with the definitions in Eq. (6), we arrive at a broadened CME (bCME) for ρ_0 and ρ_1,

$$\frac{\partial}{\partial t}\rho_0(x,p,t) = -\frac{p}{m}\frac{\partial \rho_0}{\partial x} + \frac{\partial \tilde{U}_0}{\partial x}\frac{\partial \rho_0}{\partial p} - \frac{\Gamma}{\hbar}\bar{f}\rho_0 + \frac{\Gamma}{\hbar}(1-\bar{f})\rho_1, \tag{15a}$$

$$\frac{\partial}{\partial t}\rho_1(x,p,t) = -\frac{p}{m}\frac{\partial \rho_1}{\partial x} + \frac{\partial \tilde{U}_1}{\partial x}\frac{\partial \rho_1}{\partial p} + \frac{\Gamma}{\hbar}\bar{f}\rho_0 - \frac{\Gamma}{\hbar}(1-\bar{f})\rho_1, \tag{15b}$$

where $\tilde{U}_0$ and $\tilde{U}_1$ are broadened diabatic surfaces defined as

$$\frac{\partial \tilde{U}_0}{\partial x} = \frac{\partial U_0}{\partial x} + (\bar{n} - \bar{f})\frac{\partial h}{\partial x}, \tag{16a}$$

$$\frac{\partial \tilde{U}_1}{\partial x} = \frac{\partial U_1}{\partial x} + (\bar{n} - \bar{f})\frac{\partial h}{\partial x}. \tag{16b}$$

In this paper, our goal is to benchmark Eq. (15). Note the simplicity of these equations: Such simple equations would not have resulted if our extrapolation had joined Eqs. (13) and (7b) together.

The bCME [Eq. (15)] or the CME [Eq. (4)] can be easily solved using surface hopping procedures: a swarm of trajectories running on the two potential energy surfaces with stochastic hopping between the two surfaces. Details of the surface hopping algorithm can be found in Ref. 72.

E. Observables

Below, we will compare steady state current-voltage characteristics (I-V curves) and phonon excitation for the bCME/CME against exact HQME results. A few words are appropriate regarding how we extract observables.

1. I-V curves

For the CME, in the spirit of a master equation,[72] the current is given by

$$I = \frac{e}{\hbar}\int dxdp \left(\Gamma^{\mathrm{L}} f^{\mathrm{L}}(h)\rho_0(x,p) - \Gamma^{\mathrm{L}}(1 - f^{\mathrm{L}}(h))\rho_1(x,p)\right). \tag{17}$$

For the bCME, to incorporate broadening effects into the current, we first define the local Landauer current,

$$I_{loc}(x) \equiv \frac{e}{\hbar}\int \frac{d\epsilon}{2\pi} \frac{\Gamma^{\mathrm{L}}\Gamma^{\mathrm{R}}}{(\epsilon - h(x))^2 + (\Gamma/2)^2}(f^{\mathrm{L}}(\epsilon) - f^{\mathrm{R}}(\epsilon)). \tag{18}$$

The final current is then given by averaging over the phase space distribution,

$$I = \int dxdp\, I_{loc}(x)A(x,p). \tag{19}$$

Again, $A(x,p) \equiv \rho_0(x,p) + \rho_1(x,p)$.

2. Phonon excitation

Below, we will assume that the nuclear motion is harmonic, i.e., $U_0(x) = \frac{1}{2}m\omega^2 x^2$, such that we can compare the average phonon excitation $\langle \hat{a}^\dagger \hat{a}\rangle$. By definition, $\hbar\omega(\hat{a}^\dagger\hat{a} + \frac{1}{2}) = \frac{1}{2}m\omega^2\hat{x}^2 + \frac{\hat{p}^2}{2m}$ so that we may calculate average phonon excitations in the classical regime as follows:

$$\langle \hat{a}^\dagger \hat{a}\rangle = \frac{m\omega}{2\hbar}\langle x^2\rangle + \frac{\langle p^2\rangle}{2m\omega\hbar} - \frac{1}{2}. \tag{20}$$

In the CME or bCME, $\langle x^2\rangle$ and $\langle p^2\rangle$ are given by averaging phase space distribution,

$$\langle x^2\rangle = \int dxdp\, x^2 A(x,p), \tag{21a}$$

$$\langle p^2\rangle = \int dxdp\, p^2 A(x,p). \tag{21b}$$

III. QME AND BQME

For the bCME or CME, the nuclear potential $U_0(x)$ and electron-nuclear coupling $h(x)$ are general, but results hold only at reasonably large temperature. To be able to push our results into the quantum (low temperature) limit, we will restrict ourselves to the case of harmonic oscillator and linear

coupling, such that $U_0 = \frac{1}{2}m\omega^2x^2$ and $h(x) = E_d + g\sqrt{\frac{2m\omega}{\hbar}}x$. Now we rewrite the Hamiltonian [in Eq. (1)] in terms of raising and lowering operators ($\hat{a}^\dagger$ and $\hat{a}$) instead of position and momentum operators ($\hat{x}$ and $\hat{p}$) and perform a system-bath partitioning,

$$\hat{H} = \hat{H}_\mathrm{S} + \hat{H}_\mathrm{B} + \hat{H}_\mathrm{SB} \tag{22}$$

with

$$\hat{H}_\mathrm{S} = \hat{d}\hat{d}^\dagger\hat{H}_0 + \hat{d}^\dagger\hat{d}\hat{H}_1, \tag{23a}$$

$$\hat{H}_\mathrm{B} = \sum_{k\in\mathrm{L,R}} \epsilon_k\hat{c}_k^\dagger\hat{c}_k, \tag{23b}$$

$$\hat{H}_\mathrm{SB} = \sum_{k\in\mathrm{L,R}} (V_k\hat{c}_k^\dagger\hat{d} + \mathrm{h.c.}), \tag{23c}$$

where

$$\hat{H}_0 = \hbar\omega(\hat{a}^\dagger\hat{a} + \frac{1}{2}), \tag{24a}$$

$$\hat{H}_1 = \hbar\omega(\hat{a}^\dagger\hat{a} + \frac{1}{2}) + g(\hat{a}^\dagger + \hat{a}) + E_d. \tag{24b}$$

In such a case, assuming $\Gamma < k_BT$, it is straightforward to derive a quantum master equation for the reduced density matrix $\hat{\rho}_0$ and $\hat{\rho}_1$,[73,77]

$$\begin{aligned}\frac{\partial\hat{\rho}_0}{\partial t} &= -\frac{\mathrm{i}}{\hbar}[\hat{H}_0,\hat{\rho}_0] - \sum_K\sum_{k\in K}\frac{|V_k|^2}{\hbar^2}\\ &\times\int_0^\infty d\tau e^{\mathrm{i}\epsilon_k\tau/\hbar}f^K(\epsilon_k)e^{-\mathrm{i}\hat{H}_1\tau/\hbar}e^{\mathrm{i}\hat{H}_0\tau/\hbar}\hat{\rho}_0\\ &- e^{\mathrm{i}\epsilon_k\tau/\hbar}(1-f^K(\epsilon_k))\hat{\rho}_1e^{-\mathrm{i}\hat{H}_1\tau/\hbar}e^{\mathrm{i}\hat{H}_0\tau/\hbar} + h.c.,\end{aligned} \tag{25a}$$

$$\begin{aligned}\frac{\partial\hat{\rho}_1}{\partial t} &= -\frac{\mathrm{i}}{\hbar}[\hat{H}_1,\hat{\rho}_1] - \sum_K\sum_{k\in K}\frac{|V_k|^2}{\hbar^2}\\ &\times\int_0^\infty d\tau e^{-\mathrm{i}\epsilon_k\tau/\hbar}(1-f^K(\epsilon_k))e^{-\mathrm{i}\hat{H}_0\tau/\hbar}e^{\mathrm{i}\hat{H}_1\tau/\hbar}\hat{\rho}_1\\ &- e^{-\mathrm{i}\epsilon_k\tau/\hbar}f^K(\epsilon_k)\hat{\rho}_0e^{-\mathrm{i}\hat{H}_0\tau/\hbar}e^{\mathrm{i}\hat{H}_1\tau/\hbar} + h.c.\end{aligned} \tag{25b}$$

To include broadening within the QME, similar to the bCME, we replace $\hat{H}_0/\hat{H}_1$ by the corresponding broadened $\hat{\tilde{H}}_0/\hat{\tilde{H}}_1$ in Eq. (25),

$$\begin{aligned}\frac{\partial\hat{\rho}_0}{\partial t} &= -\frac{\mathrm{i}}{\hbar}[\hat{\tilde{H}}_0,\hat{\rho}_0] - \sum_K\sum_{k\in K}\frac{|V_k|^2}{\hbar^2}\\ &\times\int_0^\infty d\tau e^{\mathrm{i}\epsilon_k\tau/\hbar}f^K(\epsilon_k)e^{-\mathrm{i}\hat{\tilde{H}}_1\tau/\hbar}e^{\mathrm{i}\hat{\tilde{H}}_0\tau/\hbar}\hat{\rho}_0\\ &- e^{\mathrm{i}\epsilon_k\tau/\hbar}(1-f^K(\epsilon_k))\hat{\rho}_1e^{-\mathrm{i}\hat{\tilde{H}}_1\tau/\hbar}e^{\mathrm{i}\hat{\tilde{H}}_0\tau/\hbar} + h.c.,\end{aligned} \tag{26a}$$

$$\begin{aligned}\frac{\partial\hat{\rho}_1}{\partial t} &= -\frac{\mathrm{i}}{\hbar}[\hat{\tilde{H}}_1,\hat{\rho}_1] - \sum_K\sum_{k\in K}\frac{|V_k|^2}{\hbar^2}\\ &\times\int_0^\infty d\tau e^{-\mathrm{i}\epsilon_k\tau/\hbar}(1-f^K(\epsilon_k))e^{-\mathrm{i}\hat{\tilde{H}}_0\tau/\hbar}e^{\mathrm{i}\hat{\tilde{H}}_1\tau/\hbar}\hat{\rho}_1\\ &- e^{-\mathrm{i}\epsilon_k\tau/\hbar}f^K(\epsilon_k)\hat{\rho}_0e^{-\mathrm{i}\hat{\tilde{H}}_0\tau/\hbar}e^{\mathrm{i}\hat{\tilde{H}}_1\tau/\hbar} + h.c.\end{aligned} \tag{26b}$$

Here $\hat{\tilde{H}}_0 = \hat{H}_0 + \Delta U(x)$ and $\hat{\tilde{H}}_1 = \hat{H}_1 + \Delta U(x)$, where $\Delta\mathrm{U}(x)$ is the shift of the two PESs,

$$\Delta U(x) = \int_{x_0}^{x} dx'\,(\bar{n}(h(x')) - \bar{f}(h(x'))\frac{\partial}{\partial x'}h(x')) \tag{27}$$

where x_0 is some reference point.

Both the bQME and QME can be further simplified using the eigenbasis of the vibrational states. In the Appendix, we show how to solve these equations and calculate the observables in practice.

IV. HIERARCHICAL QUANTUM MASTER EQUATION (HQME)

In the following, we provide some details regarding the numerically exact HQME approach which will be used to benchmark the results of our newly developed methods. The HQME approach [also known as hierarchical equation of motion (HEOM) approach] was originally proposed in the context of relaxation dynamics[80,81] and later on applied to charge transport.[69–71] We closely follow Ref. 71, where the HQME approach for a numerically exact treatment of vibrationally coupled transport was introduced.

Based on the system-bath partitioning in Eq. (22), it is numerically expedient (see the supplementary material of Ref. 71 for details) to diagonalize the Hamiltonian of the reduced system $\hat{H}_\mathrm{S}$ by employing a small polaron transformation, $\hat{\tilde{H}} = \hat{S}\hat{H}\hat{S}^\dagger$ with $\hat{S} = \exp\left((g/\hbar\omega)\left(\hat{a}^\dagger - \hat{a}\right)\hat{d}^\dagger\hat{d}\right)$. The resulting Hamiltonian is given by

$$\hat{\tilde{H}} = \hat{\tilde{H}}_\mathrm{S} + \hat{H}_\mathrm{B} + \hat{\tilde{H}}_\mathrm{SB} \tag{28}$$

with

$$\hat{\tilde{H}}_S = \tilde{E}_d\hat{d}^\dagger\hat{d} + \hbar\omega\left(\hat{a}^\dagger\hat{a} + \frac{1}{2}\right), \tag{29a}$$

$$\hat{\tilde{H}}_\mathrm{SB} = \sum_{k\in\mathrm{L,R}} (V_k\hat{X}\hat{c}_k^\dagger\hat{d} + \mathrm{h.c.}). \tag{29b}$$

The small polaron transformation leads to a renormalization of the energy of the electronic state $\tilde{E}_d = E_d - g^2/(\hbar\omega)$ and the molecule-lead coupling term is dressed by the shift operator $\hat{X} = \exp\{(g/\hbar\omega)(\hat{a} - \hat{a}^\dagger)\}$.

Employing a bath interaction picture, the bath coupling operators are defined by

$$\hat{b}_K^\sigma(t) = \exp\left(\mathrm{i}\hat{H}_\mathrm{B}t/\hbar\right)\left(\sum_{k\in K}V_k\hat{c}_k^\sigma\right)\exp\left(-\mathrm{i}\hat{H}_\mathrm{B}t/\hbar\right) \tag{30}$$

with $\sigma = \pm$, $\hat{c}_k^- \equiv \hat{c}_k$, and $\hat{c}_k^+ \equiv \hat{c}_k^\dagger$. As these operators obey Gaussian statistics, all information about system-bath coupling is encoded in the two-time correlation function of the free bath $C_K^\sigma(t-\tau) = \langle\hat{b}_K^\sigma(t)\hat{b}_K^{\bar{\sigma}}(\tau)\rangle_\mathrm{B}$, where $\bar{\sigma} \equiv -\sigma$. Via Fourier transformation

$$C_K^\sigma(t) = \frac{1}{2\pi}\int_{-\infty}^{\infty}\mathrm{d}\epsilon\,\mathrm{e}^{\sigma\mathrm{i}\epsilon t/\hbar}\Gamma^K(\epsilon)f[\sigma(\epsilon-\mu_K)], \tag{31}$$

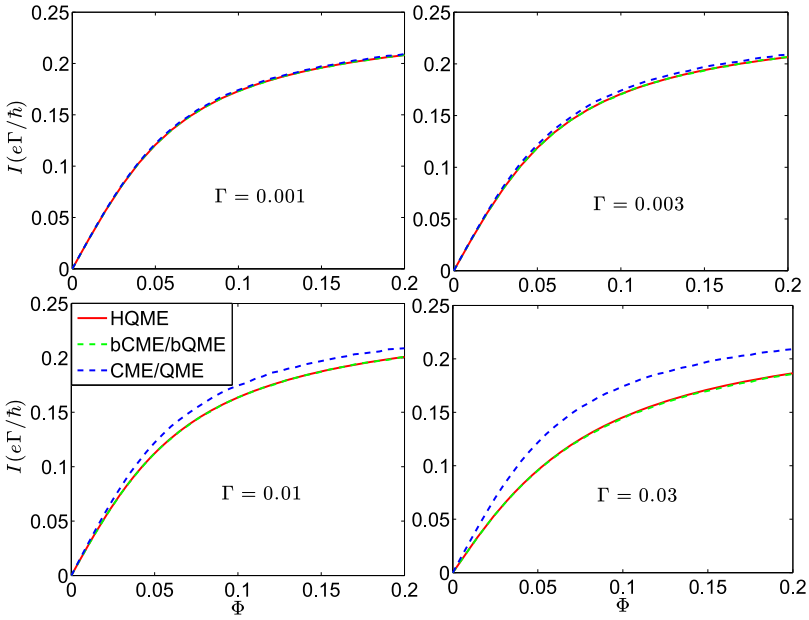

FIG. 1. I-V curves in the classical limit: $k_BT = 0.01$, $\hbar\omega = 0.003$. The bQME and bCME agree with the HQME almost exactly, whereas the QME and CME fail in the limit of large Γ. Other parameters: $g = 0.0075$, $\tilde{E}_d = 0$. $\mu_L = -\mu_R = \Phi/2$, $\Gamma_L = \Gamma_R = \Gamma/2$.

$C_K^\sigma(t)$ is related to the spectral density in the leads $\Gamma^K(\epsilon)$ and the Fermi-Dirac distribution $f(\epsilon) = (\exp(\epsilon/k_BT) + 1)^{-1}$. To derive a closed set of EOMs within the HQME method, $C_K^\sigma(t)$ is expressed by a sum over exponentials,[69] $C_K^\sigma(t) = \sum_{l=0}^{l_{\max}} \eta_{K,l} e^{-\gamma_{K,\sigma,l}t}$. To this end, the Fermi distribution is represented by a sum-over-poles scheme employing a Pade decomposition[82–84] and the spectral density of the leads is assumed to be a single Lorentzian $\Gamma^K(\epsilon) = \frac{1}{2}\frac{\Gamma W^2}{(\epsilon-\mu_K)^2+W^2}$. The bandwidth W is set to be 10^6 times larger than Γ to effectively describe the leads in the wideband limit, which implies that the overall molecule-lead coupling strength is independent of energy and symmetric, $\Gamma^L = \Gamma^R = \frac{1}{2}\Gamma$.

The HQMEs for vibrationally coupled transport are given by

$$\frac{\partial}{\partial t}\hat{\rho}^{(n)}_{j_n\cdots j_1} = -\left(\frac{\mathrm{i}}{\hbar}\hat{\tilde{\mathcal{L}}}_S + \sum_{m=1}^{n}\gamma_{j_m}\right)\hat{\rho}^{(n)}_{j_n\cdots j_1} - \frac{\mathrm{i}}{\hbar^2}\sum_j \hat{\mathcal{A}}^{\bar{\sigma}}\hat{\rho}^{(n+1)}_{jj_n\cdots j_1} - \mathrm{i}\sum_{m=1}^{n}(-)^{n-m}\hat{\mathcal{C}}_{j_m}\hat{\rho}^{(n-1)}_{j_n\cdots j_{m+1}j_{m-1}\cdots j_1}, \tag{32}$$

with the multi-index $j = (K, \sigma, l)$ and $\hat{\tilde{\mathcal{L}}}_S\hat{O} = [\hat{\tilde{H}}_S, \hat{O}]$. Here, $\hat{\rho}^{(0)} \equiv \hat{\rho}$ stands for the reduced density matrix and $\hat{\rho}^{(n)}_{j_n\cdots j_1}$ $(n > 0)$ denote auxiliary density operators, which describe bath-related observables such as, e.g., the current

$$\langle \hat{I}_K(t)\rangle = \mathrm{i}\frac{e}{\hbar}\sum_l \mathrm{Tr}_S\left\{\hat{d}\hat{X}\hat{\rho}^{(1)}_{K,+,l}(t) - \mathrm{h.c.}\right\}. \tag{33}$$

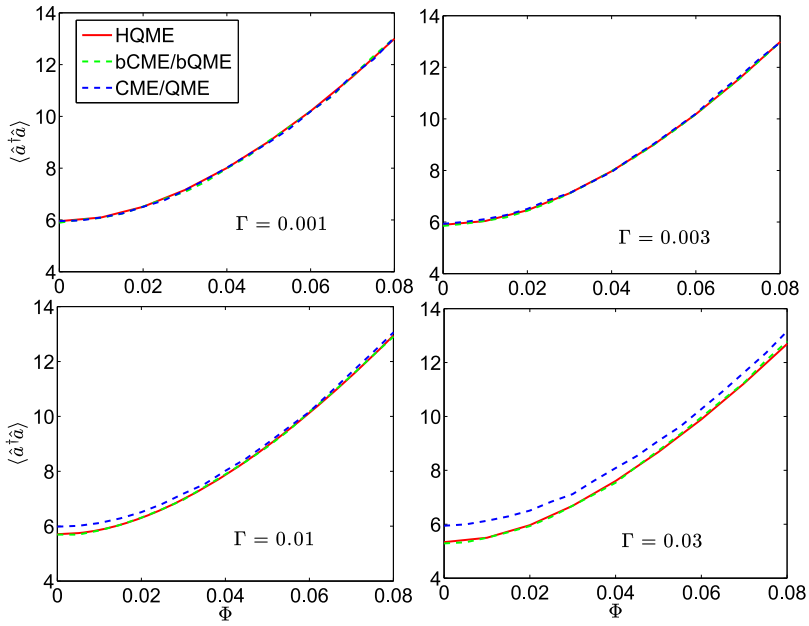

FIG. 2. Phonon excitation-voltage curves in the classical limit: $k_BT = 0.01$, $\hbar\omega = 0.003$. bQME and bCME agree with the HQME almost exactly, whereas the QME and CME fail in the limit of large Γ. Other parameters: $g = 0.0075$, $\tilde{E}_d = 0$. $\mu_L = -\mu_R = \Phi/2$, $\Gamma_L = \Gamma_R = \Gamma/2$.

The superoperators $\hat{\mathcal{A}}$ and $\hat{\mathcal{C}}$ read

$$\hat{\mathcal{A}}^{\bar{\sigma}}\hat{\rho}^{(n)} = \hat{d}^{\bar{\sigma}}\hat{X}^{\bar{\sigma}}\hat{\rho}^{(n)} + (-)^n\hat{\rho}^{(n)}\hat{d}^{\bar{\sigma}}\hat{X}^{\bar{\sigma}}, \tag{34a}$$

$$\hat{\mathcal{C}}_{K,\sigma,l}\hat{\rho}^{(n)} = \eta_{K,l}\hat{d}^{\sigma}\hat{X}^{\sigma}\hat{\rho}^{(n)} - (-)^n\eta^*_{K,l}\hat{\rho}^{(n)}\hat{d}^{\sigma}\hat{X}^{\sigma}. \tag{34b}$$

Note that, above, $\hat{d}^- \equiv \hat{d}$ (and $\hat{d}^+ \equiv \hat{d}^\dagger$) are dressed by $\hat{X}^- \equiv \hat{X}$ (and $\hat{X}^+ \equiv \hat{X}^\dagger$) due to the small polaron transformation. According to system-bath interaction, the superoperator $\hat{\mathcal{A}}$ ($\hat{\mathcal{C}}$) couples the nth level of the hierarchy to the $(n+1)$th [$(n-1)$th] level. The coupled set of equations is solved directly for the steady state by setting $\dot{\hat{\rho}}^{(n)}_{j_n\cdots j_1}(t=\infty) = 0$ $(n \geq 0)$. In the calculations presented below, the results are quantitatively converged for a truncation of the hierarchy at level $n = 3$.

The coupled set of HQMEs in Eq. (32) is evaluated in the electronic-vibrational product basis, $\langle b|\langle i_0|\hat{\rho}^{(n)}_{j_n\cdots j_1}\left|i'_0\right\rangle|b'\rangle$, where $|b\rangle \in \{|0\rangle, |1\rangle\}$ and $|i_0\rangle$ denote eigenstates of $\hat{d}^\dagger\hat{d}$ and $\hat{H}_0$ [defined in Eq. (24a)], respectively, with $b \in \{0,1\}$ and $i_0 \in \{0,\ldots,i_0^{\max}\}$. Without performing the small polaron transformation, an identical set of EOMs can be obtained if the HQMEs are evaluated in the eigenstate-basis of $\hat{H}_S$. This basis set is given by the product states $|0\rangle|i_0\rangle$ and $|1\rangle|i_1\rangle$, where $|i_1\rangle$ with $i_1 \in \{0,\ldots,i_1^{\max}\}$ denotes the eigenstates of $\hat{H}_1$ [cf. Eq. (24b)].

The results presented in Figs. 3 and 4 are obtained by the HQME approach outlined above. For the results shown in Figs. 1 and 2, an alternative HQME approach is applied where the vibration is treated as part of the bath subspace. Due to the high average vibrational excitation in the systems considered in Figs. 1 and 2, a treatment of the vibrational mode as part of the reduced system would require a huge vibrational basis set $\{0,\ldots,i_0^{\max}\}$ which is computationally not feasible.

V. RESULTS

Below, we will restrict ourselves to the symmetric case with voltage $\mu_L = -\mu_R = \Phi/2, \Gamma_L = \Gamma_R = \frac{1}{2}\Gamma$ and reorganized energy level $\tilde{E}_d \equiv E_d - g^2/(\hbar\omega) = 0$.

A. Classical regime

In this subsection, we look at the classical regime, where $k_BT > \hbar\omega$, such that a classical treatment of the nuclear motion is feasible.

For the I-V curves, as shown in Fig. 1, the bCME agrees almost perfectly with numerically exact results from HQME, regardless of whether we look at the adiabatic limit $\Gamma > \hbar\omega$ or the nonadiabatic limit $\Gamma < \hbar\omega$. Not surprisingly, if we do not incorporate broadening, in the limit that $\Gamma > k_BT$, both the CME and the QME fail to recover the correct I-V results. In this limit ($k_BT > \hbar\omega$), the quantum treatment (the QME) completely agrees with a classical treatment (i.e., the CME).

In Fig. 2, we show the results for phonon excitation, which is a property of the nuclear distribution. The agreement between the bCME and HQME indicates that in the limit of large Γ, the potential surface has to be broadened in order to recover the correct phonon distribution. Again, the (b)QME and (b)CME are completely identical.

To understand why the bCME can capture broadening effects correctly in the classical limit ($k_BT > \hbar\omega$), we note that broadening is important only when $\Gamma > k_BT$, which automatically implies that we are in the adiabatic regime $\Gamma > \hbar\omega$. Furthermore, in such an adiabatic regime, the bCME reduces to a Fokker-Planck equation with the correct potential of mean force [Eq. (11)] and a roughly correct friction tensor.[47] Thus, the bCME should be quite valid. That being said, as shown below, such a broadening scheme will not work perfectly in the quantum and nonadiabatic regimes, where $\hbar\omega > \Gamma > k_BT$, especially when k_BT is very low.

B. Quantum regime

In the highly quantum regime, where $\hbar\omega > k_BT$, Fig. 3 starts to show differences between the (b)QME with (b)CME. A classical treatment fails in this limit, whereas the bQME agrees with the numerically exact solution very well. A straightforward QME shows deviations from the HQME in the limit of larger Γ.

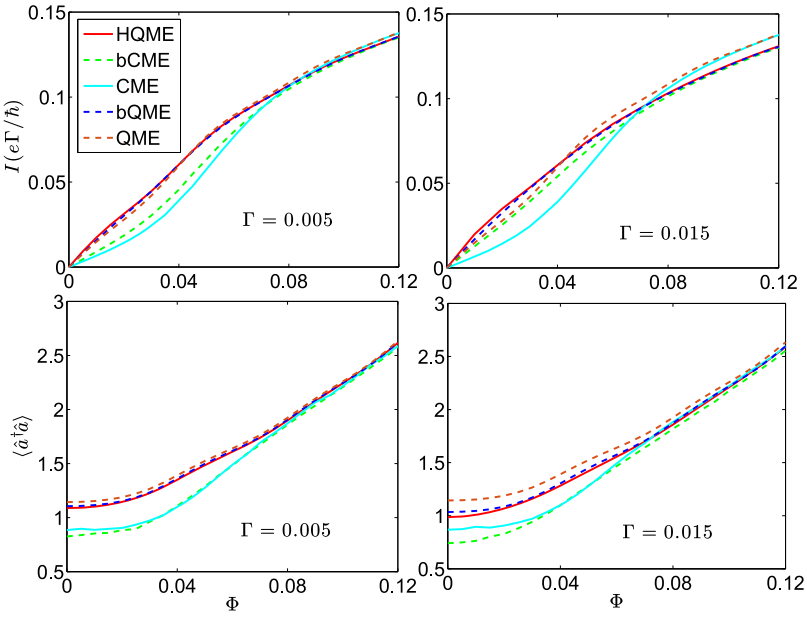

FIG. 3. Quantum regime: $k_BT = 0.005$, $\hbar\omega = 0.02$. In this limit, a classical treatment fails. Overall the bQME performs well. Other parameters: $g = 0.03$, $\tilde{E}_d = 0$. $\mu_L = -\mu_R = \Phi/2$, $\Gamma_L = \Gamma_R = \Gamma/2$.

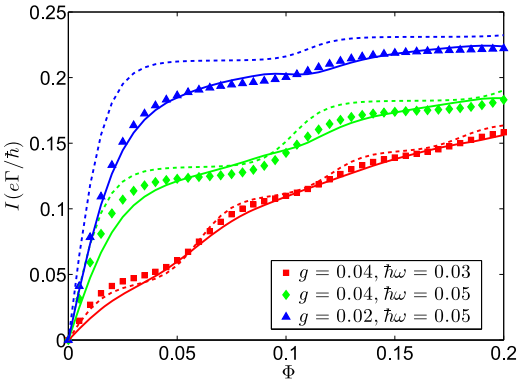

FIG. 4. Low temperature: $\Gamma = 0.01, k_BT = 0.004$. Data from the QME (dashed lines) and bQME (solid lines) are benchmarked against the HQME (squares, diamonds, and triangles). The QME data show very sharp step-like features. By contrast, the bQME data show step-like features that are much less sharp. The current from the bQME data is in closer overall agreement with the HQME, but neither the bQME nor the QME is quantitatively accurate here. $\tilde{E}_d = 0$, $\mu_L = -\mu_R = \Phi/2$, $\Gamma_L = \Gamma_R = \Gamma/2$.

Overall, the results in Fig. 3 give us a great deal of confidence that the bQME should work well both in the high temperature ($k_BT \gg \hbar\omega$) and intermediate temperature regimes ($k_BT = \hbar\omega$); by contrast, the bCME can be valid only in the high temperature limit. As discussed above, for broadening to be important, Γ must be larger than k_BT ($\Gamma > k_BT$), which again brings us back to the adiabatic regime ($\Gamma > \hbar\omega$), where the bQME should be valid. As shown in Fig. 3, the bQME works well even for the nonadiabatic and quantum regimes, $\hbar\omega > \Gamma > k_BT$, provided that k_BT is not very small compared to $\hbar\omega$.

Finally, in the highly nonadiabatic and quantum regime ($\hbar\omega \gg \Gamma \gg k_BT$), Fig. 4 shows that the I-V curves display step-like features. Compared with numerically exact results, the QME predicts very sharp step features, which is a signature of the fact that the QME lacks broadening. By contrast, the bQME predicts a less obvious step feature, though the results are not perfect. Looking forward, we cannot be sure our techniques to incorporate broadening are optimal at very low temperatures, and the data in Fig. 4 provide one set of benchmarks for further improvement of semiclassical methods. That being said, we are also not sure whether such an improved broadening technique exists given the *ad hoc* nature of our correction. For the moment, however, we are reasonably confident that the bCME/bQME is reliable at reasonable large temperatures. The next step will be to benchmark these techniques with more than one orbital in the system so that these techniques can be applied to realistic molecules near surfaces. This work is ongoing.

VI. CONCLUSION

In this paper, the broadened classical master equation (bCME) introduced previously[76] to treat coupled electron-nuclear motions at molecule-metal interfaces has been extended to the non-equilibrium case, whereby two electrodes surround the molecule and a bias voltage is applied. The bCME algorithm agrees with the numerical exact solution almost perfectly in the limit of $k_BT > \hbar\omega$. In the quantum limit, $k_BT < \hbar\omega$, an analogous broadening strategy is suggested for the QME, and the resulting bQME strategy works fairly well. That being said, at very low temperature, the I-V curves produced by the bQME yield step features that are too soft compared with exact HQME data, reminding us that there are clear limits to the validity of semiclassical approaches. Looking forward, we soon hope to test both the bCME and bQME for larger Hamiltonians with anharmonic surfaces and multiple system orbitals (beyond the limit of wideband coupling) and thus learn much more about when semiclassical dynamics can or cannot be used safely for realistic systems.

ACKNOWLEDGMENTS

M.T. and C.S. thank Rainer Härtle for insightful discussions on the HQME method. The work at Erlangen is supported by the German Research Foundation (DFG) via SFB 953 and a research grant and used resources of the computing center Erlangen (RRZE). The work at the University of Pennsylvania is supported by the (U.S.) Air Force Office of Scientific Research (USAFOSR) PECASE award under AFOSR Grant No. FA9950-13-1- 0157. J.E.S. gratefully acknowledges support from the Stanford PULSE Institute and a John Simon Guggenheim Memorial fellowship.

APPENDIX: THE QME AND BQME

Here we provide details for solving the bQME set of equations. We first express the operators $\hat{H}_0$, $\hat{H}_1$,

$$\hat{H}_0 = \hbar\omega(\hat{a}^\dagger\hat{a} + \frac{1}{2}), \tag{A1a}$$

$$\hat{H}_1 = \hbar\omega(\hat{a}^\dagger\hat{a} + \frac{1}{2}) + g(\hat{a}^\dagger + \hat{a}) + E_d \tag{A1b}$$

in the basis of eigenstates of $\hat{a}^\dagger\hat{a}$ (referred to as the boson basis), where

$$\hat{a}^\dagger\hat{a} = \begin{bmatrix} 0 & & & \\ & 1 & & \\ & & 2 & \\ & & & \ddots \end{bmatrix}, \hat{a} + \hat{a}^\dagger = \begin{bmatrix} 0 & 1 & & & \\ 1 & 0 & \sqrt{2} & & \\ & \sqrt{2} & 0 & \sqrt{3} & \\ & & \cdots & \cdots & \cdots \end{bmatrix}. \tag{A2}$$

To build matrices for $\hat{\tilde{H}}_0$ and $\hat{\tilde{H}}_1$, we need to express $\Delta U(\hat{x})$ [Eq. (27)] in the boson basis [since $\hat{\tilde{H}}_0 = \hat{H}_0 + \Delta U(\hat{x})$ and $\hat{\tilde{H}}_1 = \hat{H}_1 + \Delta U(\hat{x})$]. To do so, we diagonalize the position operator $\hat{x} = \sqrt{\frac{\hbar}{2m\omega}}(\hat{a} + \hat{a}^\dagger)$, such that $\hat{x}\,|x_i\rangle = x_i\,|x_i\rangle$, where in such a basis, $\langle x_i|\,U(\hat{x})\,\big|x_j\big\rangle = U(x_i)\delta_{ij}$. We then transform $U(\hat{x})$ back to the boson basis.

We next express the bQME [Eq. (26)] in the respective eigenbases of $\hat{\tilde{H}}_0$ and $\hat{\tilde{H}}_1$,

$$\hat{\tilde{H}}_0\,|i_0\rangle = E_{i_0}\,|i_0\rangle\,, \tag{A3a}$$

$$\hat{\tilde{H}}_1\,|i_1\rangle = E_{i_1}\,|i_1\rangle\,. \tag{A3b}$$

After a secular approximation, the bQME reads

$$\dot{\rho}_0(i_0) = -\sum_{i_1,K} W^{0\to1,K}_{i_0\to i_1}\rho_0(i_0) + \sum_{i_1,K} W^{1\to0,K}_{i_1\to i_0}\rho_1(i_1), \tag{A4a}$$

$$\dot{\rho}_1(i_1) = \sum_{i_0,K} W^{0\to1,K}_{i_0\to i_1}\rho_0(i_0) - \sum_{i_0,K} W^{1\to0,K}_{i_1\to i_0}\rho_1(i_1), \tag{A4b}$$

where

$$W^{0\to1,K}_{i_0\to i_1} = |\langle i_1|i_0\rangle|^2 \frac{\Gamma^K}{\hbar} f^K(E_{i_1} - E_{i_0}), \tag{A5a}$$

$$W^{1\to0,K}_{i_1\to i_0} = |\langle i_1|i_0\rangle|^2 \frac{\Gamma^K}{\hbar}(1 - f^K(E_{i_1} - E_{i_0})). \tag{A5b}$$

The steady state solution of the above equation is the nontrivial solution that satisfies $\dot{\rho}_0 = 0$, $\dot{\rho}_1 = 0$. When calculating the current, we use the expression

$$I = \frac{e}{\hbar}\sum_{i_0,i_1}|\langle i_1|i_0\rangle|^2 \int d\epsilon \frac{\Gamma^L\Gamma^R}{(\epsilon - (E_{i_1} - E_{i_0}))^2 + \Gamma^2} \times (f^L(\epsilon) - f^R(\epsilon))(\rho_0(i_0) + \rho_1(i_1)). \tag{A6}$$

For the unbroadened QME, we calculate the current by

$$I = e\sum_{i_0,i_1} W^{0\to1,L}_{i_0\to i_1}\rho_0(i_0) - W^{1\to0,L}_{i_1\to i_0}\rho_1(i_1). \tag{A7}$$

Finally, for calculating phonon excitations $\langle\hat{a}^\dagger\hat{a}\rangle$ within both QME and bQME, we set

$$\langle\hat{a}^\dagger\hat{a}\rangle = \sum_{i_0}\langle i_0|\hat{a}^\dagger\hat{a}|i_0\rangle\rho_0(i_0) + \sum_{i_1}\langle i_1|\hat{a}^\dagger\hat{a}|i_1\rangle\rho_1(i_1). \tag{A8}$$

The number of phonon basis states is truncated once the final results have converged.

[1] A. Nitzan and M. A. Ratner, Science **300**, 1384 (2003).
[2] A. Nitzan, Annu. Rev. Phys. Chem. **52**, 681 (2001).
[3] N. J. Tao, Nat. Nanotechnol. **1**, 173 (2006).
[4] J. Park, A. N. Pasupathy, J. I. Goldsmith, C. Chang, Y. Yaish, J. R. Petta, M. Rinkoski, J. P. Sethna, H. D. Abruña, P. L. McEuen, and D. C. Ralph, Nature **417**, 722 (2002).
[5] C. W. J. Beenakker, Phys. Rev. B **44**, 1646 (1991).
[6] M. Dorogi, J. Gomez, R. Osifchin, R. P. Andres, and R. Reifenberger, Phys. Rev. B **52**, 9071 (1995).
[7] L. Bogani and W. Wernsdorfer, Nat. Mater. **7**, 179 (2008).
[8] L. H. Yu and D. Natelson, Nano Lett. **4**, 79 (2004).
[9] A. Zhao, Q. Li, L. Chen, H. Xiang, W. Wang, S. Pan, B. Wang, X. Xiao, J. Yang, J. G. Hou, and Q. Zhu, Science **309**, 1542 (2005).
[10] W. Liang, M. P. Shores, M. Bockrath, J. R. Long, and H. Park, Nature **417**, 725 (2002).
[11] C. Romeike, M. R. Wegewijs, W. Hofstetter, and H. Schoeller, Phys. Rev. Lett. **96**, 196601 (2006).
[12] G. Cohen, E. Gull, D. R. Reichman, and A. J. Millis, Phys. Rev. Lett. **112**, 146802 (2014).
[13] J. Koch and F. von Oppen, Phys. Rev. Lett. **94**, 206804 (2005).
[14] R. Leturcq, C. Stampfer, K. Inderbitzin, L. Durrer, C. Hierold, E. Mariani, M. G. Schultz, F. von Oppen, and K. Ensslin, Nat. Phys. **5**, 327 (2009).
[15] E. Burzurí, Y. Yamamoto, M. Warnock, X. Zhong, K. Park, A. Cornia, and H. S. J. van der Zant, Nano Lett. **14**, 3191 (2014).
[16] L.-Y. Hsu, T.-W. Tsai, and B.-Y. Jin, J. Chem. Phys. **133**, 144705 (2010).
[17] M. Galperin, M. A. Ratner, A. Nitzan, and A. Troisi, Science **319**, 1056 (2008).
[18] R. Härtle and M. Thoss, in *Molecular Electronics: An Experimental and Theoretical Approach*, edited by I. Baldea (Pan Stanford, Singapore, 2015), Chap. 5, p. 155.
[19] K. Kaasbjerg, T. Novotný, and A. Nitzan, Phys. Rev. B **88**, 201405 (2013).
[20] L. Siddiqui, A. W. Ghosh, and S. Datta, Phys. Rev. B **76**, 085433 (2007).
[21] R. Härtle and M. Thoss, Phys. Rev. B **83**, 125419 (2011).
[22] R. Härtle, R. Volkovich, M. Thoss, and U. Peskin, J. Chem. Phys. **133**, 081102 (2010).
[23] R. Härtle and M. Kulkarni, Phys. Rev. B **91**, 245429 (2015).
[24] F. Reckermann, M. Leijnse, M. Wegewijs, and H. Schoeller, Europhys. Lett. **83**, 58001 (2008).
[25] T. Frederiksen, K. Franke, A. Arnau, G. Schulze, J. Pascual, and N. Lorente, Phys. Rev. B **78**, 233401 (2008).
[26] J. Repp and G. Meyer, Nat. Phys. **6**, 975 (2010).
[27] A. Erpenbeck, R. Härtle, and M. Thoss, Phys. Rev. B **91**, 195418 (2015).
[28] J. Koch, F. von Oppen, and A. V. Andreev, Phys. Rev. B **74**, 205438 (2006).
[29] D. Secker, S. Wagner, S. Ballmann, R. Härtle, M. Thoss, and H. B. Weber, Phys. Rev. Lett. **106**, 136807 (2011).
[30] C. Schinabeck, R. Härtle, H. Weber, and M. Thoss, Phys. Rev. B **90**, 075409 (2014).
[31] C. Li, D. Zhang, X. Liu, S. Han, T. Tang, C. Zhou, J. K. Wendy Fan, J. Han, M. Meyyappan, A. M. Rawlett, D. W. Price, and J. M. Tour, Appl. Phys. Lett. **82**, 645 (2003).
[32] S. W. Wu, N. Ogawa, G. V. Nazin, and W. Ho, J. Phys. Chem. C **112**, 5241 (2008).
[33] E. Lörtscher, J. W. Ciszek, J. Tour, and H. Riel, Small **2**, 973 (2006).
[34] E. Wilner, H. Wang, M. Thoss, and E. Rabani, Phys. Rev. B **89**, 205129 (2014).
[35] J. Chen, M. A. Reed, A. M. Rawlett, and J. M. Tour, Science **286**, 1550 (1999).
[36] K. Walzer, E. Marx, N. C. Greenham, R. J. Less, P. R. Raithby, and K. Stokbro, J. Am. Chem. Soc. **126**, 1229 (2004).
[37] I. Amlani, A. M. Rawlett, L. A. Nagahara, and R. K. Tsui, Appl. Phys. Lett. **80**, 2761 (2002).
[38] M. Galperin, M. Ratner, and A. Nitzan, Nano Lett. **5**, 125 (2005).
[39] R. Härtle and M. Thoss, Phys. Rev. B **83**, 115414 (2011).
[40] T. Seideman, J. Phys.: Condens. Matter **15**, R521 (2003).
[41] F. Mohn, J. Repp, L. Gross, G. Meyer, M. S. Dyer, and M. Persson, Phys. Rev. Lett. **105**, 266102 (2010).
[42] C. Hofmeister, P. Coto, and M. Thoss, J. Chem. Phys. **146**, 092317 (2017).
[43] D. Weckbecker, P. B. Coto, and M. Thoss, Nano Lett. **17**, 3341 (2017).
[44] R. Pozner, E. Lifshitz, and U. Peskin, Nano Lett. **14**, 6244 (2014).
[45] A. Mitra, I. Aleiner, and A. J. Millis, Phys. Rev. B **69**, 245302 (2004).
[46] M. Galperin, M. A. Ratner, and A. Nitzan, J. Phys.: Condens. Matter **19**, 103201 (2007).
[47] N. Bode, S. V. Kusminskiy, R. Egger, and F. von Oppen, Beilstein J. Nanotechnol. **3**, 144 (2012).
[48] T. Frederiksen, M. Paulsson, M. Brandbyge, and A.-P. Jauho, Phys. Rev. B **75**, 205413 (2007).
[49] R. Härtle, C. Benesch, and M. Thoss, Phys. Rev. B **77**, 205314 (2008).
[50] T. Novotný, F. Haupt, and W. Belzig, Phys. Rev. B **84**, 113107 (2011).
[51] L. K. Dash, H. Ness, and R. W. Godby, Phys. Rev. B **84**, 085433 (2011).
[52] Y. Utsumi, O. Entin-Wohlman, A. Ueda, and A. Aharony, Phys. Rev. B **87**, 115407 (2013).
[53] B. K. Agarwalla, J.-H. Jiang, and D. Segal, Phys. Rev. B **92**, 245418 (2015).
[54] R. Volkovich, R. Härtle, M. Thoss, and U. Peskin, Phys. Chem. Chem. Phys. **13**, 14333 (2011).
[55] M. Leijnse and M. R. Wegewijs, Phys. Rev. B **78**, 235424 (2008).
[56] J. Koch, M. Semmelhack, F. von Oppen, and A. Nitzan, Phys. Rev. B **73**, 155306 (2006).
[57] A. Erpenbeck, R. Härtle, M. Bockstedte, and M. Thoss, Phys. Rev. B **93**, 115421 (2016).
[58] M. Leijnse, M. R. Wegewijs, and K. Flensberg, Phys. Rev. B **82**, 045412 (2010).
[59] M. Brandbyge, P. Hedegård, T. F. Heinz, J. A. Misewich, and D. M. Newns, Phys. Rev. B **52**, 6042 (1995).
[60] J.-T. Lü, M. Brandbyge, P. Hedegård, T. N. Todorov, and D. Dundas, Phys. Rev. B **85**, 245444 (2012).
[61] B. Li, E. Wilner, M. Thoss, E. Rabani, and W. Miller, J. Chem. Phys. **140**, 104110 (2013).
[62] A. Jovchev and F. B. Anders, Phys. Rev. B **87**, 195112 (2013).
[63] L. Mühlbacher and E. Rabani, Phys. Rev. Lett. **100**, 176403 (2008).
[64] G. Cohen, E. Gull, D. R. Reichman, A. J. Millis, and E. Rabani, Phys. Rev. B **87**, 195108 (2013).
[65] D. Segal, A. J. Millis, and D. R. Reichman, Phys. Rev. B **82**, 205323 (2010).
[66] L. Simine and D. Segal, J. Chem. Phys. **138**, 214111 (2013).
[67] H. Wang, I. Pshenichnyuk, R. Härtle, and M. Thoss, J. Chem. Phys. **135**, 244506 (2011).
[68] H. Wang and M. Thoss, J. Chem. Phys. **145**, 164105 (2016).
[69] J. Jin, X. Zheng, and Y. Yan, J. Chem. Phys. **128**, 234703 (2008).

[70]R. Härtle, G. Cohen, D. R. Reichman, and A. J. Millis, Phys. Rev. B **88**, 235426 (2013).
[71]C. Schinabeck, A. Erpenbeck, R. Härtle, and M. Thoss, Phys. Rev. B **94**, 201407 (2016).
[72]W. Dou, A. Nitzan, and J. E. Subotnik, J. Chem. Phys. **142**, 084110 (2015).
[73]W. Dou, A. Nitzan, and J. E. Subotnik, J. Chem. Phys. **142**, 234106 (2015).
[74]W. Dou and J. E. Subotnik, J. Chem. Theory Comput. **13**, 2430 (2017).
[75]W. Dou, A. Nitzan, and J. E. Subotnik, J. Chem. Phys. **143**, 054103 (2015).
[76]W. Dou and J. E. Subotnik, J. Chem. Phys. **144**, 024116 (2016).
[77]F. Elste, G. Weick, C. Timm, and F. von Oppen, Appl. Phys. A **93**, 345 (2008).
[78]W. Dou and J. E. Subotnik, J. Chem. Phys. **146**, 092304 (2017).
[79]W. Dou and J. E. Subotnik, J. Chem. Phys. **145**, 054102 (2016).
[80]Y. Tanimura and R. Kubo, J. Phys. Soc. Jpn. **58**, 101 (1989).
[81]Y. Tanimura, J. Phys. Soc. Jpn. **75**, 082001 (2006).
[82]T. Ozaki, Phys. Rev. B **75**, 035123 (2007).
[83]J. Hu, R.-X. Xu, and Y. Yan, J. Chem. Phys. **133**, 101106 (2010).
[84]J. Hu, M. Luo, F. Jiang, R.-X. Xu, and Y. Yan, J. Chem. Phys. **134**, 244106 (2011).